Chemical Geology 426 (2016) 60–70

Contents lists available at ScienceDirect

Chemical Geology

journal homepage: www.elsevier.com/locate/chemgeo

Calcium isotopic fractionation during travertine deposition under different hydrodynamic conditions: Examples from Baishuitai (Yunnan, SW China)

Hao Yan [a,b,c], Anne-Désirée Schmitt [b,d,*], Zaihua Liu [a,**], Sophie Gangloff [b], Hailong Sun [a], Jiubin Chen [a], François Chabaux [b]

[a] State Key Laboratory of Environmental Geochemistry, Institute of Geochemistry, Chinese Academy of Sciences, Guiyang 550081, China
[b] Université de Strasbourg et CNRS, Laboratoire d'Hydrologie et de Géochimie de Strasbourg, Ecole et Observatoire des Sciences de la Terre, 1, rue Blessig, 67084, Strasbourg Cedex, France
[c] University of Chinese Academy of Sciences, Beijing 100049, China
[d] Laboratoire Chrono-environnement UMR CNRS 6249, Univ. Bourgogne Franche-Comté, F-25000 Besançon, France

ARTICLE INFO

Article history:
Received 7 April 2015
Received in revised form 23 October 2015
Accepted 1 February 2016
Available online 6 February 2016

Keywords:
Travertine
Ca isotopes
Precipitation rates
Kinetic fractionation

ABSTRACT

Revealing the potential of Ca isotopes in the research of travertine formation processes is the principal goal of this study. To achieve this, the hydrochemistry, travertine precipitation rates, and variations in Ca isotopic compositions ($\delta^{44/40}$Ca) of present-day endogenic (thermogenic) travertine in two different hydrodynamic systems (canal and pool) are studied at Baishuitai (Yunnan, SW China). In the canal, where the travertine precipitation is faster, $\delta^{44/40}$Ca values of both solution and travertine show a downstream increase, with Ca isotopic fractionation ($\Delta^{44/40}Ca_{CaCO3\text{-}aq}$) equal to ~−1.6‰. Compared to the canal, Ca isotopic fractionation between travertine and aqueous Ca^{2+} is smaller ($\Delta^{44/40}Ca_{CaCO3\text{-}aq} \approx -1.2$‰) in the pools where travertine precipitation rates are lower. The spatial variations in $\delta^{44/40}$Ca values of solution and travertine are related to the amount of Ca removed from the solution when $\delta^{44/40}$Ca values of spring water remain stable. In addition, the results confirm the control of precipitation rates on Ca isotopic fractionation between calcite and parent aqueous Ca^{2+} using natural samples. The observed negative correlation between $\Delta^{44/40}Ca_{CaCO3\text{-}aq}$ and travertine precipitation rates can be explained by the steady-state kinetic surface reaction model proposed by DePaolo (2011), with equilibrium and kinetic fractionation factors of $\alpha_{eq} = 1.0000 \pm 0.0001$ and $\alpha_f = 0.9983 \pm 0.0002$, respectively. An important consequence of this study is that Ca isotopes in travertine systems are good tools to have access to variations of $\delta^{44/40}Ca_{aq}$, which are directly linked to the amount of precipitated Ca. This could then be useful for reconstructing past hydrodynamic conditions when applied to travertine core data.

1. Introduction

Speleothems, tufa and travertine are widespread terrestrial carbonates that form in caves, lakes, and rivers/streams, respectively, and are among the most important continental climate-related deposits (Ford and Pedley, 1996; Pentecost, 2005; Liu et al., 2006; Jones and Renaut, 2010). Their deposition is controlled by several factors, such as CO_2 degassing due to inorganic or organic processes. Travertine and tufa consist of microgranular calcite, which result from two main formation processes: (1) $CaCO_3$ encrusts filamentous microbionts, whose biannual laminations reflect seasonal changes in the water chemistry, cyanobacterial growth and/or hydrology of the depositional environment (Chafetz et al., 1991; Matsuoka et al., 2001; Andrews and Brasier, 2005; Kano et al., 2007; Kawai et al., 2009), and (2) $CaCO_3$ forms in an endogenic (thermogenic) way with multiple CO_2 sources, including the hydrolysis and oxidation of reduced carbon, decarbonatation of limestone, or direct contributions from the deep crust or upper mantle (Ford and Pedley, 1996; Minissale et al., 2002; Crossey et al., 2009). Due to high growth rates (mm to cm per year), travertine has unique advantages in providing high-resolution (up to seasonal, monthly or even daily) palaeoclimatic and palaeoenvironmental information (Kano et al., 2003; Liu et al., 2010).

Palaeoenvironmental changes can be recorded in travertine via variations in lamina thickness, textures, trace element concentrations and their stable isotope compositions (Ihlenfeld et al., 2003). Oxygen (O) and carbon (C) isotopic compositions (δ^{18}O and δ^{13}C, respectively) are by far the most commonly investigated paleo-proxies in travertine (Andrews, 2006; Kano et al., 2007). However, it is difficult to unambiguously relate directly the measured isotopic variations in travertine to

* Correspondence to: A.-D. Schmitt, Université de Strasbourg et CNRS, Laboratoire d'Hydrologie et de Géochimie de Strasbourg, Ecole et Observatoire des Sciences de la Terre, 1, rue Blessig, 67084, Strasbourg Cedex, France.
** Corresponding author.
E-mail addresses: adschmitt@unistra.fr (A.-D. Schmitt), liuzaihua@vip.gyig.ac.cn (Z. Liu).

http://dx.doi.org/10.1016/j.chemgeo.2016.02.002
0009-2541/

specific environmental changes. For instance, $\delta^{18}O$ values of travertine formed in different hydrodynamic environments may show similar seasonal trends, where one is due to the temperature variation and the other to the dilution by rainfall (Wang et al., 2014). A potential approach to solve this problem is to employ combined isotopic systems so that various environmental information can be separated from each other. Though calcium (Ca) is one of the main elements in travertine, little or no data have been reported so far on variation in its isotopic compositions.

Ca isotope fractionation during inorganic $CaCO_3$ precipitation (calcite and aragonite) has been primarily studied for a decade via several laboratory experiments (Gussone et al., 2003; Lemarchand et al., 2004; Marriott et al., 2004; Gussone et al., 2005; Tang et al., 2008; Gussone et al., 2011; Reynard et al., 2011; Tang et al., 2012). In contrast, few studies dealt with continental carbonate field samples (Tipper et al., 2006; Nielsen and DePaolo, 2013). Tipper et al. (2006) reported results on travertine from the southern Tibetan Plateau and showed that those travertine were isotopically light compared to surrounding river water and limestone samples. More recently, Nielsen and DePaolo (2013) studied tufa that precipitated from supersaturated lake water in Mono Lake (California) and observed that the intensity of Ca isotopic fractionation depends on the solution chemistry, with variations that are consistent with the theoretical model proposed by the authors for the formation of those carbonates.

Here, we focus on the endogenic travertine-depositing canal and pools of Baishuitai (Yunnan, SW China), a natural laboratory to study isotopic fractionation associated with calcite precipitation. Some of previous studies at this site attempted to understand seasonal variations in the hydrochemistry, $CaCO_3$ precipitation rates and formation of biannual laminae in the canal and to discuss their climatic implications (Liu et al., 2003, 2006, 2010). Other studies dealt with the C and O isotope ratios in modern travertine from the canal and the pools (Liu et al., 2006; Sun and Liu, 2010; Yan et al., 2012; Sun et al., 2014). In the present study, we aim 1) to determine the variations in $\delta^{44/40}Ca$ values of present-day travertine and their controlling factors, 2) to test if the precipitation rate dependence of Ca isotope fractionation between calcite and solution found in the laboratory could also be observed in naturally travertine-depositing systems, and 3) to discuss the potential of Ca isotopes applied to travertine.

2. General Settings of the study

The Baishuitai travertine site (N27°300′, E100°02′) is located ~100 km south of Shangri-La Town, Yunnan Province, China. The elevation ranges from 2380 to 3800 m asl. The area is characterised by a subtropical monsoon climate, with >75% of the annual precipitation (~750 mm) occurring during the rainy season from May to October. The annual mean air temperature is 8 °C (Liu et al., 2003).

Baishuitai has a typical karst landscape and features one of the largest travertine deposits in China, which formed due to calcite-supersaturated aqueous solutions. Baishuitai spring water originates from the mixing of infiltrated rainfall and groundwater flow. An endogenic CO_2 source dissolves limestone from the Triassic Beiya Formation. When the spring emerges, a huge quantity of CO_2 at a high internal partial pressure is released to the atmosphere. This process creates an increase in the calcite saturation index of the water, thereby leading to $CaCO_3$ precipitation (Liu et al., 2003).

There are two travertine-depositing systems at Baishuitai: a fast-flowing canal system and a slow-flowing pool system (Fig. 1). In the canal system, a spring water rich in HCO_3^- and Ca^{2+} (S1-3) emerges from a middle Triassic limestone aquifer and mixes with a small amount of surface water from the Baishui River, which contains lower concentrations of Ca^{2+} and HCO_3^- (Liu et al., 2010; Yan et al., 2012) (Fig. 1c). Then, the mixed water flows along an ~2.5-km-long artificial canal that descends from 2900 to 2600 m asl and is accompanied by intense travertine deposition. The width of the canal ranges from 30 to 70 cm and its depth varies from 10 to 20 cm. The flow rate in the canal varies between 50 and 100 L/s.

The pools system is part of a set of large travertine terraces, which are chiefly supplied by two springs (S1-1 and S1-2, Fig. 1b). In this study, only S1-1 is studied because the hydrochemistry of the two springs is almost identical and is stable throughout the year (Sun et al., 2014). The pools are 50 to 250 cm wide, 100 to 400 cm long, and 10 to 40 cm deep. Most of the pools are located approximately 300 m (along the flow path) from the springs (S1-1 and S1-2) and have an elevation of approximately 2555 m (Fig. 1b) (for more details, see Yan et al., 2012).

3. Sampling and analytical techniques

3.1. Sampling and sample description

Two field sampling campaigns, summer 2010 and winter 2011/2012, were conducted to evaluate seasonal variations in Ca isotopic compositions. Plexiglass substrates with the dimensions 5 cm × 5 cm × 0.5 cm were placed in the flowing water (at 2–5 cm depth, in the middle of the canal or pools where water flows fast to hamper accumulation of upper calcite particles on the downward substrates) at eight different sites: Five sites (W1–W5) were selected at approximately equal intervals along the sample canal, and three sites (P4, P4.5 and P5) were chosen in three different pools (Fig. 1). The substrates were replaced every 10 days at the same locations. The travertine samples were collected from the substrates to measure the precipitation rates and stable isotopic compositions of Ca.

During each travertine sample collection, related water samples were also sampled and stored after filtration in acid-cleaned polyethylene bottles. Additionally, S1-1 and S1-3 spring waters were collected in summer 2010 and winter 2011/2012. The spring water of S1-3 corresponds to a mixture of spring and Baishui River water because it was not possible to collect pure spring water. A winter rainwater sample ~200 m away from the travertine terraces and a summer sample from the Baishui River near the S1-3 sampling location were analysed. In summer, an overland flow that contributes to the canal was also collected. A limestone sample from the middle Triassic aquifer was used to constrain the Ca isotopic composition of the bedrock.

3.2. Methods

3.2.1. Hydrochemical measurements

For each water sample (including rainwater and the S1-1 and S1-3 spring waters), the pH, water temperature, dissolved oxygen concentration (DO) and electrical conductivity (SpC) were measured in situ with a hand-held water quality meter (WTW 350i) with accuracies of ±0.05 pH units, ±0.1 °C, ±0.05 mg/L and ±0.5%, respectively. The instrument was calibrated prior to use with pH 7 and pH 10 buffers. The concentrations of HCO_3^- and Ca^{2+} were titrated on site via an Aquamerck® Alkalinity Test and Hardness Test with analytical resolutions of approximately ±6 and ±1 mg/L, respectively.

To measure the chemistry more accurately and perform Ca isotope analysis, water samples at the sampling sites were collected in acid-cleaned polyethylene bottles and filtered through 0.45 μm Minisart® filters. A non-acidified water aliquot was used for major element concentration measurements and analysed at the State Key Laboratory of Environmental Geochemistry of the Institute of Geochemistry, Chinese Academy of Sciences. The concentrations of Na^+, K^+, and Mg^{2+} were determined via an inductively coupled plasma optical emission spectrometer (ICP-OES) with an RSD of less than 5%, and the concentrations of SO_4^{2-} and Cl^- were determined by ion chromatography (Dionex® ICS-90) with RSDs of less than 2% and 4%, respectively. Another aliquot of the waters was acidified to pH < 1 via ultrapure HNO_3 for Ca isotope analyses and refrigerated.

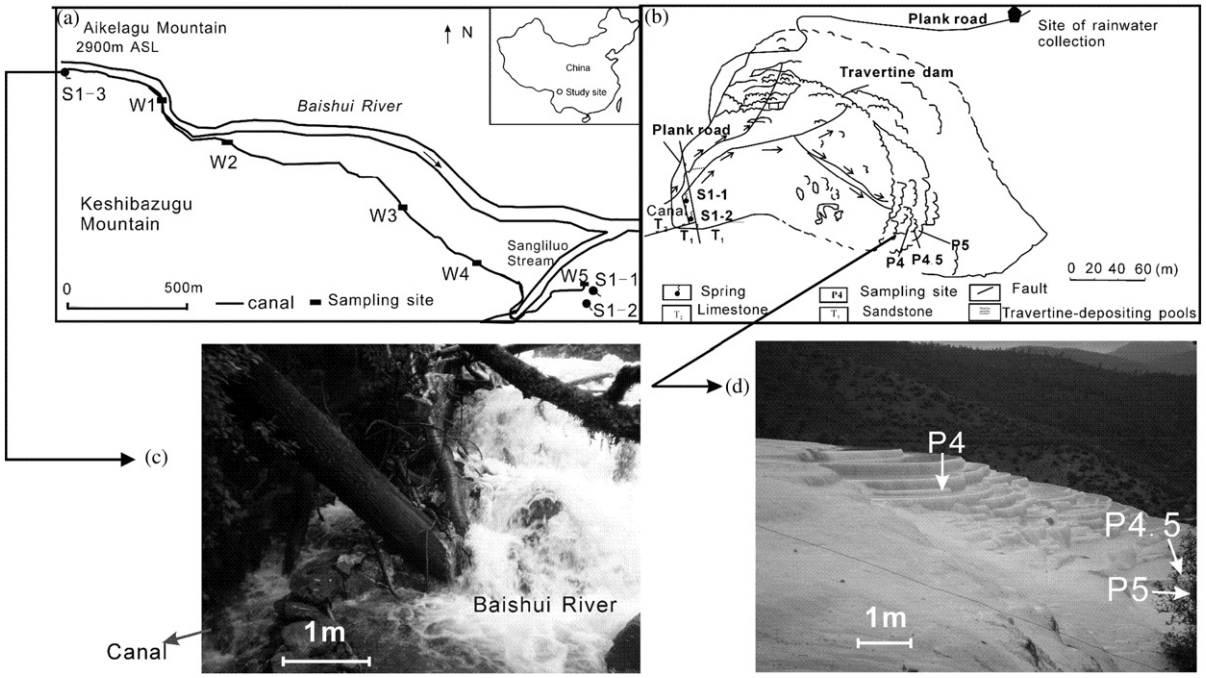

Fig. 1. (a) Distribution of the sampling sites in the travertine-depositing canal and (b) pools systems of Baishuitai (Yunnan, SW China). Note: there is a bridge (an aqueduct) for the canal between site W4 and W5, so it crosses the stream. Photos of (c) the spring S1-3, the water feeding the canal (a mixture of groundwater and Baishui River water), and (d) the pools.

The measurements of water temperature, pH and concentrations of Ca^{2+}, HCO_3^-, K^+, Na^+, Mg^{2+}, Cl^- and SO_4^{2-}, were processed with PHREEQC program (Parkhurst and Appelo, 1999) to calculate activities of CO_3^{2-}, CO_2 partial pressure (pCO_2), and calcite saturation index (SI_C).

3.2.2. Measurement of modern travertine precipitation rates and mineralogy analysis

The amount of modern travertine deposited on the plexiglass substrates was determined by measuring the weight increase of the substrates. Before immersion and after collection, each plexiglass substrate was dried at 50 °C for a period of 48 h and weighed. The carbonate precipitation rate (R_p) was calculated using the following equation:

$$R_p = (W_{ts} - W_s)/(S \times t) \quad (1)$$

where W_{ts} and W_s are the weight of the plexiglass substrates after and before each collection, respectively, t is the exposure time available for travertine to precipitate on the plexiglass substrate in each run (~10 days). It is assumed that the surface for precipitation (S) is roughly estimated as the total surface area of the substrate (60 cm^2) (Liu et al., 2010; Yan et al., 2012).

Two travertine samples from W1 and P4 were selected to be analysed by X-Ray Diffraction (XRD). Scanning electron microscopy (SEM) measurements were also performed to confirm the crystal shapes.

3.2.3. Analysis of Ca isotopic compositions

All chemical preparations and Ca isotopic analyses were performed under clean-room laboratory conditions at the Laboratoire d'Hydrologie et de Géochimie de Strasbourg (LHyGeS), following the techniques developed in the laboratory (Schmitt et al., 2009, 2013). To extract the Ca of the travertine for isotopic analysis, ~100 to 300 mg of collected travertine samples were leached with H_2O_2 (30%) to remove any organic matter before leaching the sample in 0.5 N HCl. The sample was then centrifuged and the residue was discarded. This procedure avoided any clay contribution. Approximately 150 mg of crushed limestone bedrock powder was dissolved in Savillex® vials in a procedure involving three acids (distilled HNO_3, Suprapur® HF, and Suprapur® $HClO_4$) and evaporated until dry. The water samples were evaporated in Teflon (PFA) beakers and digested with distilled HNO_3 and 30% Suprapur® H_2O_2. Once evaporated, all samples were dissolved in 1 N HNO_3.

A $^{42}Ca/^{43}Ca$ double spike (0.4 μg; $^{42}Ca/^{43}Ca$ spike ratio = 2.5) was added to the Ca from the sample (5.6 μg) and evaporated to dryness before Ca purification via high-selectivity automated ion chromatography on a Dionex® ICS-3000 device with a high-capacity carboxylate-functionalised column (Dionex® CS16). The collected Ca fractions were evaporated and re-dissolved in 2 μL 0.25 N HNO_3 and loaded without any further treatment onto a single out-gassed and partial-vacuum-oxidised Ta filament (99.995% purity). The Ca isotopic compositions were measured by thermal ionisation mass spectrometry (TIMS) using a Triton instrument (Thermo-Fisher) operating in dynamic multi-collection mode following the method described in Schmitt et al. (2009, 2013).

The Ca isotope values are expressed as a per-mil deviation relative to the NIST SRM 915a standard solution:

$$\delta^{44/40}Ca = \left\{ \left(^{44}Ca/^{40}Ca\right)_{sample} / \left(^{44}Ca/^{40}Ca\right)_{SRM915a} - 1 \right\} \times 1000 \quad (2)$$

(Eisenhauer et al., 2004).

The fractionation factor α_{CaCO3_aq} is defined as the ratio of $^{44}Ca/^{40}Ca$ of the calcite (travertine) divided by the ratio of the solution:

$$\alpha_{CaCO3-aq} = R_{CaCO3}/R_{aq}. \quad (3)$$

The calcium isotope fractionation between calcite (travertine) and the solution is expressed as

$$\Delta^{44/40}Ca_{CaCO3-aq} = \delta^{44/40}Ca_{CaCO3} - \delta^{44/40}Ca_{aq} \approx 1000 * \ln\left(\alpha_{CaCO3-aq}\right). \quad (4)$$

The external reproducibility of $\delta^{44/40}Ca$ values is 0.09‰ (2SD) based on repeated measurements of the NIST SRM 915a and on replicate sample measurements (N = 90). To improve the statistical significance of a single $\delta^{44/40}Ca$ measurement, the Ca isotope data are generally a

combination of two individual measurements, including Ca purification by ion chromatography and TIMS analyses. The accuracy of the measurements was tested by measurements of seawater during the same period of time (1.92 ± 0.08‰, 2SD; N = 8), and the values were in good agreement with previously published values (Hippler et al., 2003). Total Ca blanks for the isotope analyses were less than 3%, and blank corrections were not necessary.

4. Results

4.1. Inorganic travertine precipitation

According to the XRD results, the travertine collected by substrates consists of pure calcite without any traces of other phases, such as vaterite or aragonite. Fig. 4 shows the SEM images of travertine samples after 10 days of immersion. No macroscopic algal filament or biofilm is observed between crystals. Therefore, the deposition of well-defined calcite rhombohedra is suggested to be primarily controlled by inorganic chemical processes. Another argument pointing to inorganic travertine precipitation are the concentrations of DO in stream water. They range from 0.17 to 0.25 mmol/L (Table. EA.1). No obvious diurnial variation in concentration is observed. This suggests that photosynthesis, which consumes CO_2 and produces O_2 can be neglected, and that inorganic chemical processes are dominant in both systems. Moreover, even if some traces of organic matter should be present in the travertine samples, it should rather be derived from geogenic sources and not formed in situ, as suggested by Liu et al. (2010), which would not impact Ca isotopes.

4.2. Hydrochemical data and travertine precipitation rates

Measured and calculated hydrochemical parameters in the canal and pool systems are given in Table 1 and Figs. 2 and 3. In the two systems, the spring waters S1-3 and S1-1 have high pCO_2 values and are slightly saturated with respect to calcite (Fig. 2d–e and Fig. 3d–e). As the water flows to site W1 in the canal, pCO_2 drops to ~200 Pa, in both winter and summer in the canal and activities of CO_3^{2-} and SI_C increase to ~50 μmol/L and ~1.4 respectively due to intense degassing of CO_2, leading to travertine precipitation (Table 1). Similarly, as the water flows to P4 in the pool system, pCO_2 drops to 611 Pa in summer and 351 Pa in winter and activities of CO_3^{2-} and SI_C increase to ~40 μmol/L and 1.3 respectively. Then, the pCO_2, activities of CO_3^{2-} and SI_C values of the water remain relatively constant, although the pCO_2 of the water is much higher than that of earth's atmosphere (about 39 Pa) (Fig. 2d and Fig. 3d). The pH values follow the variations in SI_C: 6.9 and 6.7 for S1-3 and S1-1, respectively, increasing to 8.4 and 8.1, respectively, later on (Table 1; Fig. 2b and Fig. 3b). In contrast, Ca^{2+} (Fig. 2c and Fig. 3c) and HCO_3^- concentrations (Table 1) decrease from upstream to downstream because of travertine precipitation along the canal and in the pools. In the canal, water temperature increases from upstream to downstream in summer but decreases in winter (Fig. 2a). This pattern is related to seasonal variations in atmospheric temperatures. The temperatures within the pools are generally more constant for a given season (Fig. 3a; Table 1), which is certainly due to the long residence time of the water in the pools. In both the canal and the pools, the pH (only for the pools), SI_C, and SpC values and the Ca^{2+} and HCO_3^- concentrations are higher in winter than in summer certainly due to dilution effects in summer. Similarly, the smaller variations of Ca^{2+} and HCO_3^- concentrations in the pools than in the canal, could be also explained by a lower influence of the dilution effects in the pools compared to the canal (Table 1; Fig. 2c; Fig. 3c) (Sun and Liu, 2010; Liu et al., 2010; Sun et al., 2014).

The measured precipitation rates of travertine ($\log R_p$) are presented in Table 2. The rates are overall lower in the pools than in the canal (−6.25 ± 0.25, 2SD, N = 5, and −5.38 ± 0.36, 2SD, N = 10, respectively).

4.3. Ca isotopic compositions of solution, bedrock and travertine samples

The Ca isotopic compositions of the water and travertine samples ($\delta^{44/40}Ca_{aq}$ and $\delta^{44/40}Ca_{CaCO3}$, respectively) are listed in Tables 3 and 4. The collected water samples exhibit a large range of $\delta^{44/40}Ca$ values (0.25 to 1.19‰). The overland flow has the lowest $\delta^{44/40}Ca$ value (0.25 ± 0.12‰) among the water samples. The Ca isotopic composition of the rainwater sample (0.79 ± 0.06‰) is close to that of the carbonate bedrock (0.87 ± 0.06‰). The $\delta^{44/40}Ca$ value of the Baishui River water (0.67 ± 0.06‰) is slightly lower than that of the bedrock. The headwaters of the two travertine-depositing systems (S1-3 and S1-1) have the same Ca isotopic composition (~0.53‰), which is isotopically lighter

Table 1
Hydrochemical compositions of the canal and pool waters from Baishuitai travertine site.

Site	Sampling date	Water temp.[a] (°C)	pH[a]	SpC[a] (μs/cm)	Ca^{2+}[a] (mmol/L)	HCO_3-[a] (mmol/L)	CO_3^{2-}[b] (μmol/L)	pCO_2[c] (Pa)	SI_C[c]	I[c] (mmol/L)
Canal system										
S1-3	28–07-2010	7.9	6.94	650	3.75	7.39	2.10	4850	0.09	12.64
	28–01–2012	7.0	6.93	898	5.10	9.95	2.65	6542	0.30	16.17
W1	28–07-2010	8.9	8.25	630	3.65	7.16	41.10	222	1.36	12.06
	28–01–2012	6.5	8.28	853	4.83	9.44	53.04	260	1.56	15.70
W2	28–07-2010	9.7	8.33	615	3.55	7.00	49.10	180	1.43	11.54
	28–01–2012	6.2	8.36	820	4.65	9.10	60.50	207	1.61	14.56
W3	28–07-2010	12.2	8.43	566	3.30	6.46	60.41	134	1.50	10.69
	28–01–2012	5.4	8.44	725	4.10	8.05	63.00	153	1.58	12.79
W4	28–07-2010	12.9	8.41	534	3.13	6.11	55.97	137	1.45	10.22
	28–01–2012	5.0	8.44	675	3.80	7.49	58.28	143	1.52	11.98
W5	28–07-2010	14.0	8.34	496	2.90	5.70	46.30	153	1.35	9.73
	28–01–2012	4.7	8.39	620	3.50	6.90	47.94	150	1.40	11.44
Pool system										
S1-1	28–07-2010	11.0	6.7	1032	6.03	11.39	1.19	13,053	0.23	19.83
	28–01–2012	11.0	6.77	1033	5.65	11.15	2.28	10,857	0.27	18.80
P4	28–07-2010	14.7	7.93	770	4.48	8.92	28.71	611	1.30	14.91
	28–01–2012	6.2	8.16	877	4.83	9.56	40.57	351	1.44	16.43
P4.5	28–01–2012	5.5	8.24	820	4.53	8.97	44.78	273	1.46	15.17
P5	28–07-2010	15.0	8.05	679	3.90	8.03	34.40	422	1.32	13.50
	28–01–2012	5.7	8.26	811	4.48	8.89	46.67	255	1.47	15.11

[a] average values during travertine collection period.
[b] activity of CO_3^{2-} which is calculated using PHREEQC program and data from Table EA.2.
[c] calculated CO_2 partial pressure, calcite saturation index and ionic strength of water using PHREEQC program and data from Table EA.2.

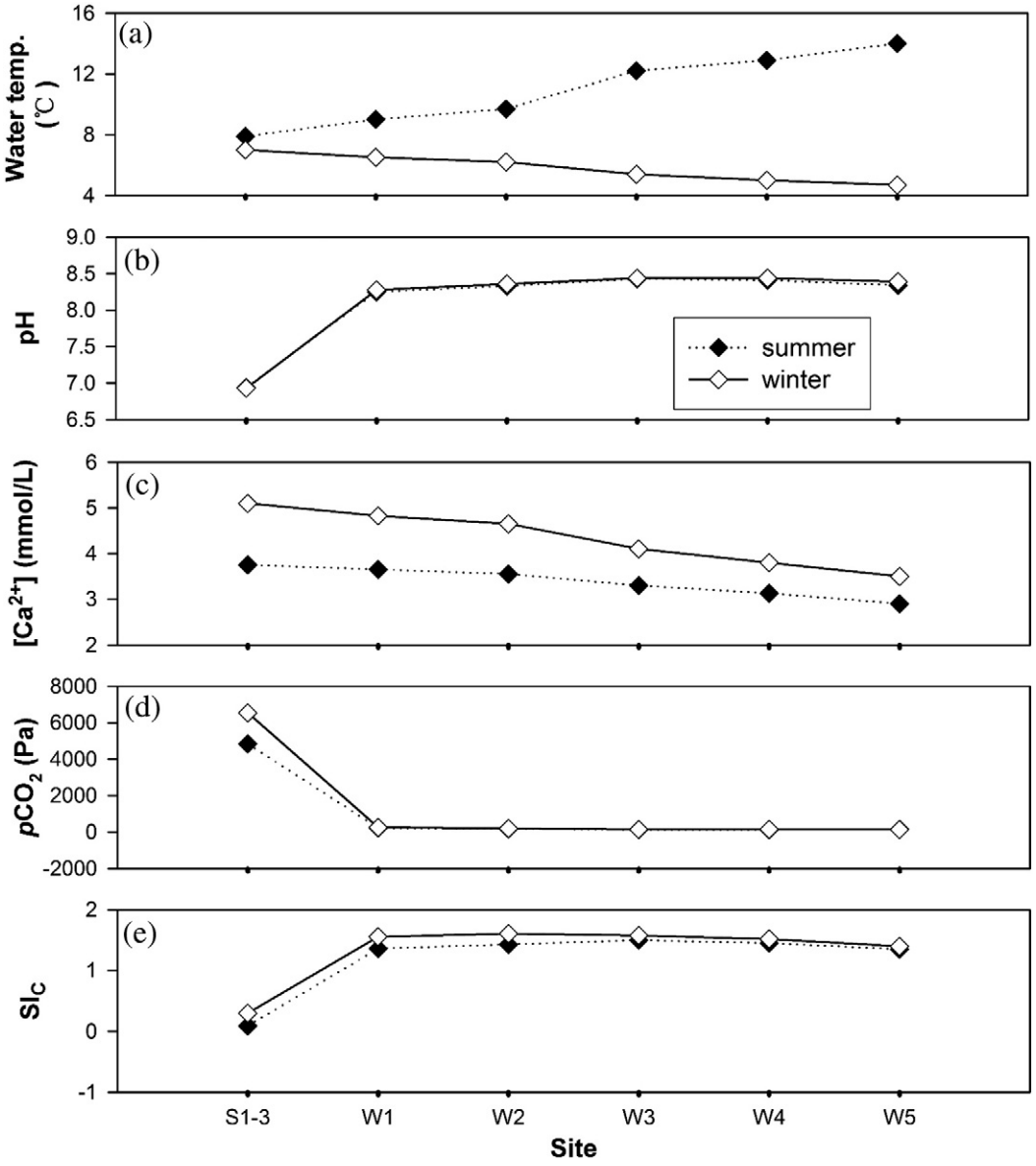

Fig. 2. Downstream evolution of (a) water temperature, (b) pH, (c) calcium concentration, (d) pCO_2 and (e) SI_C along the canal in summer and winter.

than the bedrock and rainwater. Similar ranges of variation in $\delta^{44/40}Ca_{aq}$ values are recorded in the canal and in the pools (Table 3).

All travertine samples are enriched in ^{40}Ca compared to the parent solution, which is in accord with previous experimental studies on carbonate precipitates (Gussone et al., 2003, 2005; Lemarchand et al., 2004; Tang et al., 2008; Reynard et al., 2011). The $\delta^{44/40}Ca$ values of travertine samples from the canal vary from −0.97 to −0.50‰, and the pool travertine samples are enriched in ^{44}Ca (between −0.30 and 0.01‰) compared to the canal samples. A general increase of $\delta^{44/40}Ca$ values is observed from upstream to downstream, both in the canal and in the pools, and between water and travertine samples (Fig. 5). No clear seasonal variation could be observed in travertine nor in water samples (Fig. 5).

In the canal, the $\Delta^{44/40}Ca_{CaCO3\text{-}aq}$ values range from −1.71 to −1.42‰, with a mean value of −1.58 ± 0.06‰ (2SE, N = 10; Table 3). In contrast, in the pools, Ca isotopic fractionations between travertine and aqueous Ca^{2+} are smaller, and vary from −1.38 to −1.11‰, with a mean $\Delta^{44/40}Ca_{CaCO3\text{-}aq}$ value of −1.25 ± 0.09‰ (2SE, N = 5; Table 3).

While the $\Delta^{44/40}Ca_{CaCO3\text{-}aq}$ values at Baishuitai show no obvious dependence on temperature (R^2 = 0.04), they define a negative correlation with $\log R_p$ values (Fig. 6). This variation trend is consistent with the Ca isotopic data obtained by Tang et al. (2008) in their experimental precipitation study. The trend observed in our data, which corresponds to travertine precipitation within an annual temperature range of 5 to 15 °C, is located between the two linear trends defined by Tang's experimental data at 5 and 25 °C. Our data also define negative correlations between $\Delta^{44/40}Ca_{CaCO3\text{-}aq}$ and pH (−1.08‰/pH unit; R^2 = 0.74) (not shown) and between $\Delta^{44/40}Ca_{CaCO3\text{-}aq}$ and activities of CO_3^{2-} (−0.01‰/μmol/L; R^2 = 0.55) (not shown). Because in this study $[Ca^{2+}] \gg [CO_3^{2-}]$ (see Table 1), the precipitation rate is limited by the delivery of carbonate ions, not calcium ions (Zuddas and Mucci, 1994). Thus the correlation between $\Delta^{44/40}Ca_{CaCO3\text{-}aq}$ and pH and $[CO_3^{2-}]$ is essentially the same with that of $\Delta^{44/40}Ca_{CaCO3\text{-}aq}$ and precipitation rates.

5. Discussion

5.1. Ca isotopic fractionation versus mixing processes

The increase in Ca isotopic ratios of both systems (the canal and the pools) from upstream to downstream in the stream water (Fig. 5),

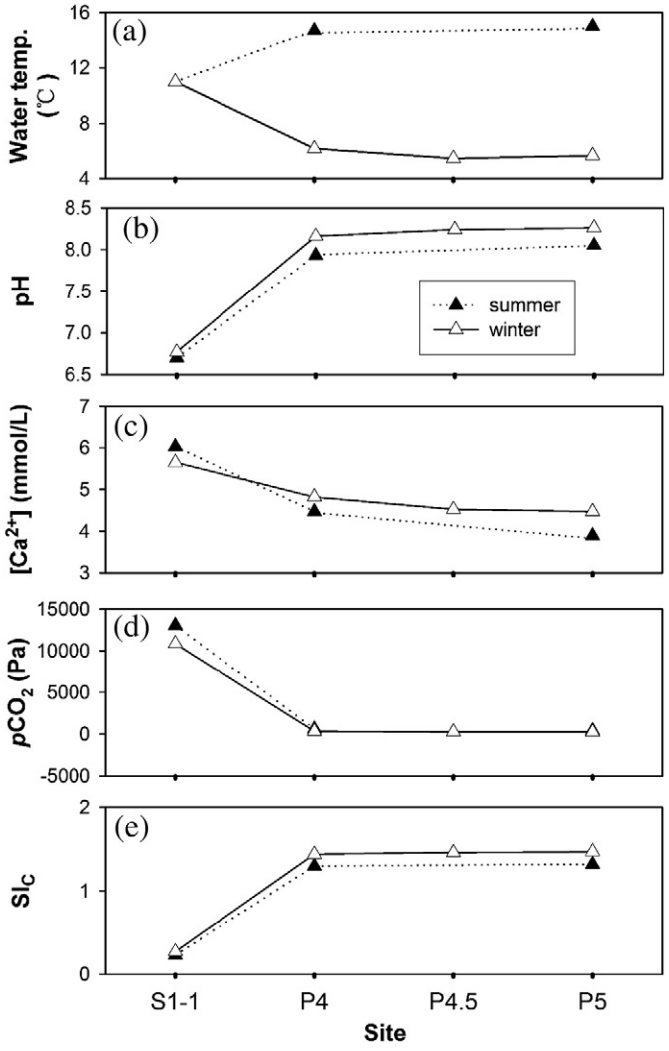

Fig. 3. Downstream evolution of (a) water temperature, (b) pH, (c) calcium concentration, (d) pCO_2 and (e) SI_C in the pool system in summer and winter.

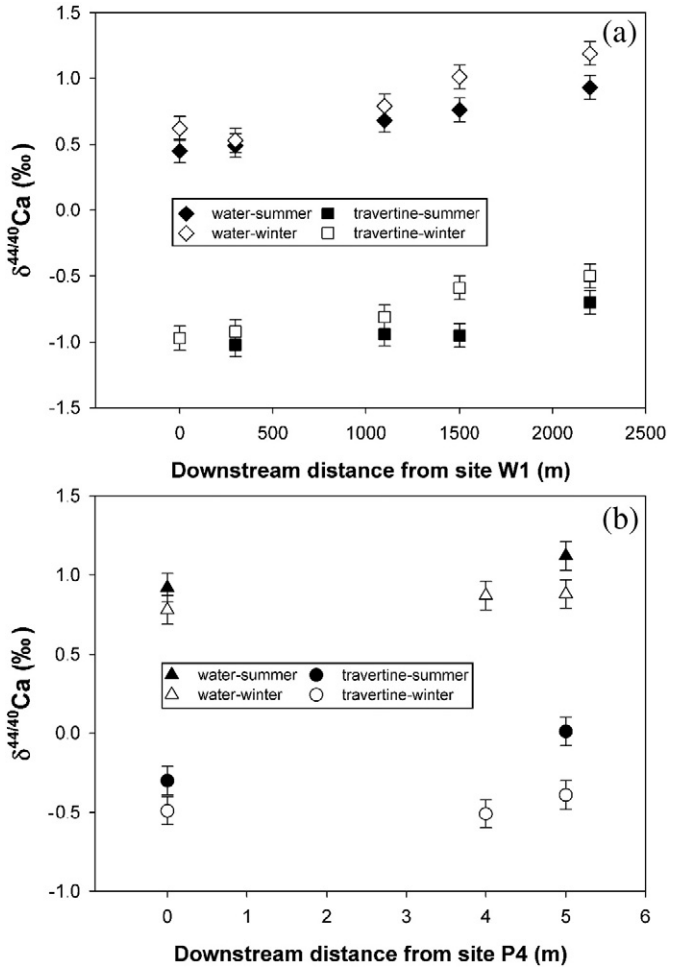

Fig. 5. Variations of $\delta^{44/40}Ca$ values of modern travertine collected in (a) the canal and (b) pools at Baishuitai in summer 2010 and winter 2011, and corresponding water samples. The Ca isotope measurement uncertainties are within the data point.

especially the positive correlation between $\delta^{44/40}Ca_{aq}$ values and the inverse of the Ca^{2+} concentrations ($1/[Ca^{2+}]$) (Fig. 7) might be simply interpreted in terms of binary mixing between two different Ca end-members, i.e., an upstream one with low $\delta^{44/40}Ca_{aq}$ and high Ca^{2+} concentration values, corresponding to the different spring waters feeding the canal and the pools, and a downstream one with higher $\delta^{44/40}Ca_{aq}$ and lower Ca concentration values. To test such a scenario, several potential calcium end-members (S1-1 and S1-3 spring waters, Baishui River, rainwater, plain overflow, and limestone bedrock) were analysed with regard to Ca concentrations and Ca isotope ratios. Although rainwater has a high $\delta^{44/40}Ca$ value (0.79 ± 0.08‰), its Ca concentration (9.8 ppm) is quite low compared with other surface waters and cannot be considered a high $\delta^{44/40}Ca$ end-member. Apart from rainwater, overland flow may also contribute to the Ca isotopic composition of canal waters in the rainy season. However, this component features the lowest $\delta^{44/40}Ca$ value (0.25 ± 0.12‰) among all the water samples. The mixing of overland flow with stream water will decrease rather than increase the $\delta^{44/40}Ca_{aq}$ values along the canal and pools. Consequently, the $\delta^{44/40}Ca_{aq}$ versus ($1/[Ca^{2+}]$) trends observed in canal and pool waters from upstream to downstream do not represent mixing process but

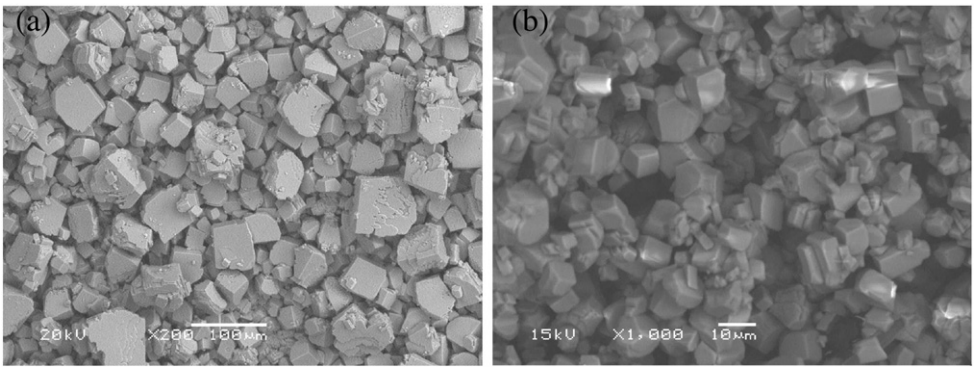

Fig. 4. SEM images showing the authigenic calcite crystals deposited on the substrate surface at W1 (a) and P4 (b).

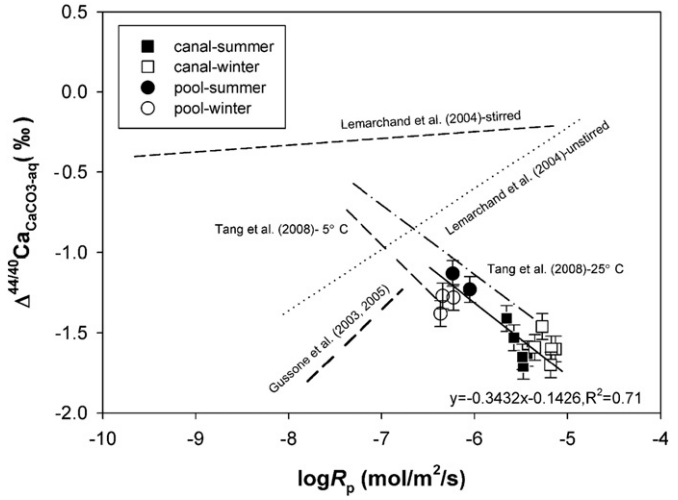

Fig. 6. $\Delta^{44/40}Ca_{calcite\text{-}aq}$ values versus precipitation rates ($\log R_p$) for present study and previous experimental studies.

represent instead isotopic fractionation associated with travertine precipitation. As a result, lighter isotopes are preferentially removed from the solution, enriching the solution in heavy Ca^{2+} isotopes. This is consistent with experimental studies (Gussone et al., 2003, 2005; Lemarchand et al., 2004; Tang et al., 2008; Reynard et al., 2011). Thus, carbonate precipitation readily accounts for downstream variations in the $\delta^{44/40}Ca$ values of the solution and travertine along the canal and pools (Fig. 5).

At this stage, the only trend that could be explained as a mixing trend would be the one defined by the spring water. Indeed, in

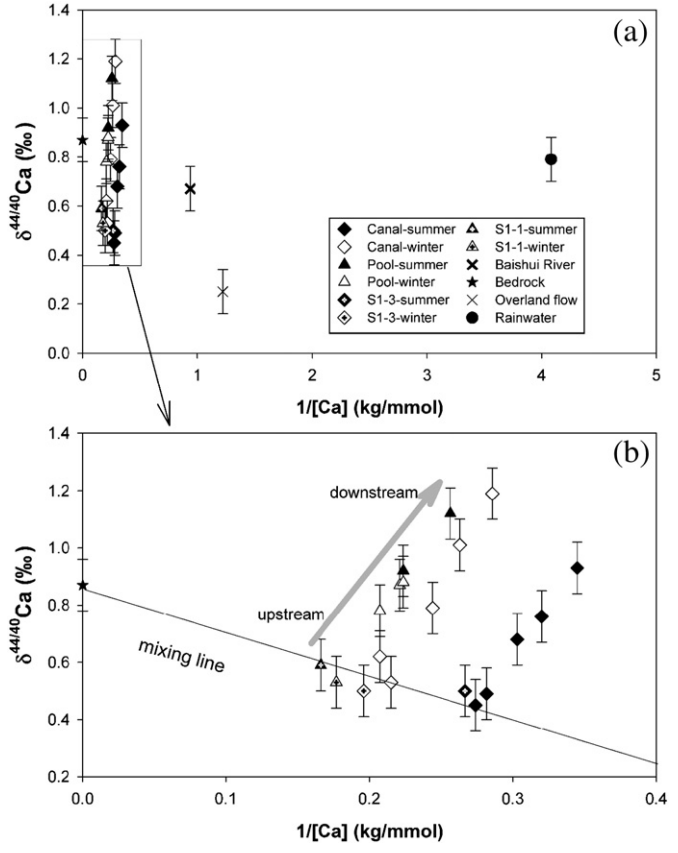

Fig. 7. $\delta^{44/40}Ca$ values versus $1/[Ca^{2+}]$ (a) for water samples and bedrock from Baishuitai travertine site; (b) close-up for spring, stream and bedrock samples.

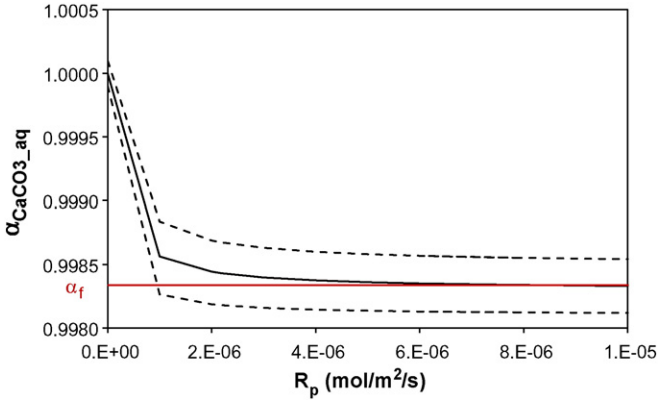

Fig. 8. α_{CaCO3_aq} variation in function of R_p (mol/m^2/s).

a $\delta^{44/40}Ca$ versus $(1/[Ca^{2+}])$ diagram, the spring water data plot along a straight line, with one end-member close to the values measured in the limestones, suggesting a potential Ca flux from the dissolution of deep limestones without any isotopic fractionation (Fig. 7b), as classically observed in mineral dissolution experiments (Ryu et al., 2011; Cobert et al., 2011). Such a mixing scenario requires the involvement of a second end-member with low $\delta^{44/40}Ca$ values and low Ca concentrations, which could not be identified from the current dataset.

5.2. Modelling of Ca isotopic fractionation

In literature, various theoretical models were employed to explain Ca isotopic fractionation in association with carbonate mineral precipitation, including kinetic models associated with aquo complex diffusion (Gussone et al., 2003, 2005), equilibrium fractionation (Marriott et al., 2004), equilibrium fractionation overprinted by kinetic effects (Lemarchand et al., 2004), adsorption-controlled steady-state (Fantle and DePaolo, 2007), surface entrapment (SEMO, Tang et al., 2008), and macroscopic and microscopic kinetic surface effects (DePaolo, 2011; Nielsen et al., 2012).

Due to the consistency between our data and those from Tang et al. (2008) (Fig. 6), the Ca isotopic fractionation in association with carbonate mineral precipitation at Baishuitai could be modelled by the surface entrapment model (SEMO, Watson, 2004), as initially applied by Tang et al. (2008) to interpret their experimental data. More recently, Tang et al.'s (2008) data have been successfully modelled using macroscopic and microscopic kinetic surface models (DePaolo, 2011; Nielsen et al., 2012). These models can be viewed as an extension of the steady-state box model from Fantle and DePaolo (2007) to explain Ca isotopic fractionation during calcite growth for a wide range of precipitation rates. The macroscopic kinetic surface model is based on the competition between the calcite growth rate and the rate of molecular exchange between the mineral surface and solution (DePaolo, 2011). It sounds reasonable to describe the actual situation of calcite growth by considering the rate of backward reaction (dissolution) comparable to precipitation rate, as suggested by many previous studies when pH > 7 (e.g., Plummer et al., 1978; Chou et al., 1989). In addition, the macroscopic parameters such as precipitation/dissolution rates which are involved in DePaolo's model can be measured or estimated in this study. Thus, we attempt to test this model with present-day field data from the canal and the pools at Baishuitai.

In this model, assuming mineral precipitation is a steady-state condition, the surface reaction-controlled condition, α_{CaCO3_aq}, can be expressed as follows (DePaolo, 2011):

$$\alpha_{CaCO_3-aq} = \frac{\alpha_f}{1 + \left(\frac{R_b}{R_p + R_b}\right)\left(\frac{\alpha_f}{\alpha_{eq}} - 1\right)} \quad (5)$$

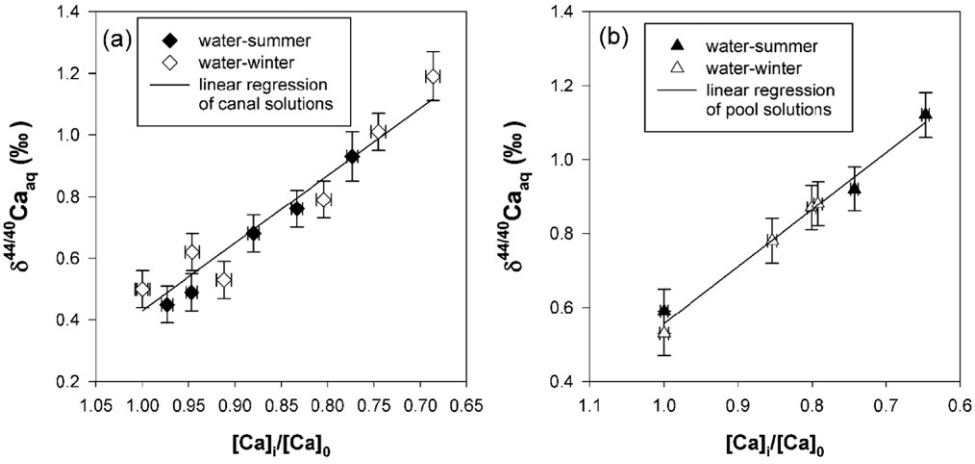

Fig. 9. $\delta^{44/40}Ca_{aq}$ versus $[Ca]_i/[Ca]_0$ for water samples from (a) the canal and (b) the pools. The regression equations are $\delta^{44/40}Ca_{aq} = -2.18(\pm0.18) \times [Ca]_i/[Ca]_0 + 2.62(\pm0.16)$, $R^2 = 0.94$, $P < 0.0001$, $N = 12$ and $\delta^{44/40}Ca_{aq} = -1.54(\pm0.08) \times [Ca]_i/[Ca]_0 + 2.10(\pm0.07)$, $R^2 = 0.99$, $P < 0.0001$, $N = 7$ for the canal and pools water samples respectively.

where α_{CaCO3_aq} is the effective isotopic fractionation factor for precipitation, α_{eq} is the equilibrium isotopic fractionation factor and α_f is the kinetic fractionation factor associated with precipitation. The parameter R_p represents the net calcite precipitation rate (i.e., the difference between precipitation and dissolution) which is estimated according to Eq. (1), and R_b represents the calcite dissolution rate (Table 2, discussed hereafter).

The calcite dissolution is usually described by the following three parallel reactions occurring at the mineral/water interface under ambient conditions but with different predominance domains (see Plummer et al., 1978; Chou et al., 1989 for more details).

$$CaCO_{3(s)} + H^+ \leftrightarrow Ca^{2+} + HCO_3^- \quad (6)$$

$$CaCO_{3(s)} + H_2CO_3 \leftrightarrow Ca^{2+} + 2HCO_3^- \quad (7)$$

$$CaCO_{3(s)} \leftrightarrow Ca^{2+} + CO_3^{2-} \quad (8)$$

Following Plummer et al. (1978) and Chou et al. (1989), the calcite dissolution rates R_b can be expressed by a sum of three terms, where each term corresponds to the dissolution rate of one of the three above reactions:

$$R_b = k_1(H^+) + k_2(H_2CO_3) + k_3 \quad (9)$$

In this equation, the parentheses denote activities and k_1, k_2 and k_3 are the temperature-dependent kinetic reaction constants of the three parallel reactions, corresponding to Eqs. (6), (7) and (8), respectively. At the condition of pH > 6 and $pCO_2 < 0.01$ atm, the third term representing the rate of surface hydration is predominant (Pokrovsky et al., 2009). In our study, the pH of stream water ranges between 7.93 and 8.44, and the pCO_2 values range between 1.1×10^{-3} and 5.0×10^{-3} atm. The dissolution rate R_b can therefore be approximated by the third term of Eq. (9), i.e., $R_b \approx k_3$.

In this context, Chou et al. (1989) determined an empirical relationship between k_3 (R_b) and pH at 25 °C. Using this experimental relationship, for the pH range of the Baishuitai waters (and more broadly for a pH range between 7.5 and 9), R_b is constant and equal to 6×10^{-7} mol/m^2/s at 25 °C (Chou et al., 1989; DePaolo, 2011). DePaolo (2011) also calculated R_b values equal to 1.55×10^{-6} mol/m^2/s at 40 °C and 1.5×10^{-7} mol/m^2/s at 5 °C for solutions with pH values varying

Table 2
Compilation of field R_p and α_{CaCO3_aq}, and calculated R_b and a_f values.

Site	Date	Field data		Calculated data	
		logR_p (mol/m^2/s)	α_{CaCO3_aq} [a]	R_b [b] (mol/m^2/s)	α_f [c]
Canal system					
W1	28–07-2010	−5.66 ± 0.1	0.99858	1.67(±0.08)E-07	0.99847
	28–01–2012	−5.35 ± 0.5	0.99841	1.54(±0.03)E-07	0.99836
W2	28–07-2010	−5.58 ± 0.1	0.99849	1.75(±0.09)E-07	0.99839
	28–01–2012	−5.28 ± 0.5	0.99855	1.53(±0.03)E-07	0.99851
W3	28–07-2010	−5.43 ± 0.1	0.99838	2.07(±0.15)E-07	0.99829
	28–01–2012	−5.13 ± 0.5	0.99840	1.53(±0.02)E-07	0.99837
W4	28–07-2010	−5.48 ± 0.1	0.99829	2.19(±0.15)E-07	0.99818
	28–01–2012	−5.18 ± 0.5	0.99840	1.53(±0.02)E-07	0.99836
W5	28–07-2010	−5.49 ± 0.1	0.99837	2.40(±0.18)E-07	0.99825
	28–01–2012	−5.18 ± 0.5	0.99831	1.53(±0.03)E-07	0.99827
Pool system					
P4	28–07-2010	−6.05 ± 0.1	0.99878	2.55(±0.20)E-07	0.99843
	28–01–2012	−6.23 ± 0.1	0.99873	1.53(±0.03)E-07	0.99840
P4.5	28–01–2012	−6.37 ± 0.1	0.99862	1.53(±0.03)E-07	0.99813
P5	28–07-2010	−6.24 ± 0.1	0.99889	2.61(±0.24)E-07	0.99839
	28–01–2012	−6.35 ± 0.1	0.99873	1.53(±0.02)E-07	0.99830

[a] Calculated from Eq. (4).
[b] Calculated from Eq. (10).
[c] Calculated from Eq. (5), α_{eq} is set to be 1.0000 ± 0.0001.

Table 3
Ca isotopic compositions of travertine and associated solution in the canal and pool systems at Baishuitai in July 2010 and January 2012.

Site No.	Sampling date	Solution			Travertine			$\Delta^{44/40}Ca_{CaCO3\text{-}aq}$ (‰)	2 SD[a] (‰)
		$\delta^{44/40}$Ca-1(‰)	$\delta^{44/40}$Ca-2(‰)	$\delta^{44/40}$Ca-avg. (‰)	$\delta^{44/40}$Ca-1(‰)	$\delta^{44/40}$Ca-2(‰)	$\delta^{44/40}$Ca-avg. (‰)		
Canal system									
S1-3	28–07-2010	0.41	0.59	0.50	-	-	-	-	-
	28–01–2012	0.47	0.52	0.50	-	-	-	-	-
W1	28–07-2010	0.42	0.48	0.45	−0.92	−1.02	−0.97	−1.42	0.13
	28–01–2012	0.58	0.65	0.62	−0.94	−1.00	−0.97	−1.59	0.13
W2	28–07-2010	0.50	0.47	0.49	−0.99	−1.06	−1.02	−1.51	0.13
	28–01–2012	0.48	0.58	0.53	−0.88	−0.97	−0.92	−1.45	0.13
W3	28–07-2010	0.67	0.69	0.68	−0.90	−0.99	−0.94	−1.62	0.13
	28–01–2012	0.82	0.75	0.79	−0.81	−0.82	−0.81	−1.60	0.13
W4	28–07-2010	0.73	0.78	0.76	−0.96	−0.94	−0.95	−1.71	0.13
	28–01–2012	1.04	0.97	1.01	−0.57	−0.61	−0.59	−1.60	0.13
W5	28–07-2010	0.93	-	0.93	−0.74	−0.67	−0.70	−1.63	0.13
	28–01–2012	1.15	1.22	1.19	−0.52	−0.49	−0.50	−1.69	0.13
Pool system									
S1-1	28–07-2010	0.63	0.54	0.59	-	-	-	-	-
	28–01–2012	0.53	0.52	0.53	-	-	-	-	-
P4	28–07-2010	0.86	0.98	0.92	−0.25	−0.36	−0.30	−1.22	0.13
	28–01–2012	0.85	0.7	0.78	−0.49	−0.50	−0.49	−1.27	0.13
P4.5	28–01–2012	0.86	0.87	0.87	−0.46	−0.56	−0.51	−1.38	0.13
P5	28–07-2010	1.03	1.21	1.12	0.08	−0.06	0.01	−1.11	0.13
	28–01–2012	0.94	0.82	0.88	−0.35	−0.43	−0.39	−1.27	0.13

[a] The error in $\Delta^{44/40}Ca_{CaCO3\text{-}aq}$ is calculated by error propagation according to the way used by Harouaka et al. (2014).

from 7.5 to 9. A polynomial regression based on the above three R_b values for 5, 25 and 40 °C yields the following empirical relationship between R_b and T:

$$R_b = 0.011667 \times T^2 - 6.4985 \times T + 906.44 \quad (10)$$

with T in Kelvin and R_b in 10^{-7} mol/m^2/s. R_b values can therefore be estimated for the different temperatures recorded at Baishuitai and are reported in Table 2.

For the calculation of α_f field R_p values and the estimated R_b values are used. α_{eq} is taken equal to 1.0000 ± 0.0001 since two field studies found the equilibrium fractionation factor equal to this value when calcite is precipitated in any system at equilibrium (Fantle and DePaolo, 2007; Jacobson and Holmden, 2008). In doing so, we obtain an average α_f equal to 0.9983 ± 0.0002 (2SD; N = 15) (Table 2). These values are similar (within the error bars) to those obtained by DePaolo (2011) to fit the experimental data of Tang et al. (2008) with their model (α_{eq} = 0.9998; α_f = 0.9983). These values are also similar (within the error bars) to those calculated by Nielsen and DePaolo (2013) (α_{eq} = 0.9998; α_f = 0.9986 ± 0.0009) to explain their field data obtained from a high-alkalinity lake system (Mono lake, California) using the microscopic $CaCO_3$ precipitation model from Nielsen et al. (2012).

Consequently, even if the number of case studies is limited, these observations might indicate that kinetic and equilibrium isotopic fractionation factors associated with calcite precipitation can be considered to be constants with known values in a wide range of carbonate precipitating systems. The immediate corollary of this conclusion is that for the common solution of $[Ca^{2+}] \gg [CO_3^{2-}]$, $\alpha_{CaCO3\text{-}aq}$ (and thus $\Delta_{CaCO3\text{-}aq}$, see Eqs. (4) would be only dependent on two main parameters: T and R_p (see Eqs. (5) and (10)). In the specific case of the Baishuitai carbonates, the absence of a clear correlation between $\Delta^{44/40}Ca_{CaCO3\text{-}aq}$ and temperature accounts for the observation that $\Delta^{44/40}Ca_{CaCO3\text{-}aq}$ is predominantly influenced by calcite precipitation rates and not dominated by seasonal temperature changes due to small temperature variation (a maximum of 10 °C). This result is consistent with the small temperature-dependence of $\Delta^{44/40}Ca_{CaCO3\text{-}aq}$ observed in the laboratory during calcite precipitation experiments (between 0.014 and 0.02‰/°C; Marriott et al., 2004; Tang et al., 2008; Reynard et al., 2011).

5.3. Geochemical implications

When considering Eq. (5) and applying data obtained in Section 5.2 (i.e. α_{eq} = 1.0000 ± 0.0001; α_f = 0.9983 ± 0.0002; R_b = (18.3 ± 8.3) × 10^{-8} mol/m^2/s), one observes that α_{CaCO3_aq} is not much variable and tends to α_f (Fig. 8). This implies that the fractionation is dominated by the kinetic fractionation factor associated to precipitation (DePaolo, 2011). In this case, following Eq. (4), $\Delta^{44/40}Ca_{CaCO3\_aq}$ tends to −1.70 ± 0.17 ‰. If one considers $\Delta^{44/40}Ca_{CaCO3\_aq}$ as being constant, then, following Eq. (4), a variation of $\delta^{44/40}Ca_{CaCO3}$ has to be linked to a variation of $\delta^{44/40}Ca_{aq}$.

The immediate consequence of this result is, that $\delta^{44/40}Ca_{aq}$ values of the solution follow a Rayleigh fractionation, which can be expressed as

$$\delta^{44/40}Ca_{aq-i} = \left(1000 + \delta^{44/40}Ca_0\right)\left([Ca]_i/[Ca]_0\right)^{\alpha(CaCO3-aq)-1} - 1000 \quad (11)$$

where $\delta^{44/40}Ca_0$ and $\delta^{44/40}Ca_{aq\text{-}i}$ are Ca isotopic compositions of solution at spring (S1-3 or S1-1) and site i respectively, while $[Ca]_0$ and $[Ca]_i$ are calcium concentrations at spring (S1-3 or S1-1) and site i, respectively.

Since the $\delta^{44/40}Ca$ values of spring water ($\delta^{44/40}Ca_0$) are stable throughout the year (Table 3) and the fractionation factor $\alpha_{CaCO3\text{-}aq}$ is rather constant (Table 2 and Fig. 8), the amount of Ca removed from the solution ($[Ca]_i/[Ca]_0$) is the main factor that controls $\delta^{44/40}Ca_{aq}$ (Fig. 9).

Table 4
Calcium isotopic compositions and concentrations of overland flow, rainwater, Baishui River and bedrock samples at Baishuitai.

Sample	Sampling date	[Ca] (mmol/kg)	$\delta^{44/40}$Ca-1(‰)	$\delta^{44/40}$Ca-2(‰)	$\delta^{44/40}$Ca-avg.(‰)
Overland flow	22–06-2010	0.82	0.25	-	0.25
Rainwater	04–01–2012	0.24	0.79	0.78	0.79
Baishui River	28–07-2010	1.07	0.67	0.66	0.67
Bedrock	28–01–2012	5484	0.86	0.88	0.87

Table EA.1
Concentration of dissolved O_2 in spring and stream water measured by WTW350i on site in summer 2010.

Site	DO (mmol/L)			Site	DO (mmol/L)		
	Morning	Noon	Evening		Morning	Noon	Evening
S1-3	0.23	0.23	0.23	S1-1	0.04	0.04	0.04
W1	0.25	0.25	0.24	P4	0.22	0.19	0.18
W2	0.25	0.25	0.24	P5	0.21	0.18	0.17
W3	0.25	0.24	0.24	P6	0.21	0.18	0.18
W4	0.24	0.24	0.23				
W5	0.25	0.23	0.23				

Another consequence of this study is that Ca isotopic compositions applied to past travertine samples should give information on past variations on the surrounding water hydrology, variations that are directly linked to the precipitation rate of the travertine. Such $\delta^{44/40}Ca_{CaCO3}$ variations in travertine cores could be due to different calcium sources or to variations in the distance from the Ca source of water, which would result in local different compositions of the fluid. To answer this question, the analysis of calcite samples from different core profiles, as well as the use of source tracers such as $^{87}Sr/^{86}Sr$ isotopes (Hori et al., 2013) could be helpful. Combining Ca isotopes with C and O isotopes could also give information on water temperature, water chemistry and/or precipitation rates variations (Dietzel et al., 2009; Yan et al., 2012; Sun et al., 2014; Wang et al., 2014). Moreover, in order to determine if potential isotopic variations are local or regional, and to compare them to the results of other studies, it is necessary to determine the chronometric framework of the samples by dating them, using ^{14}C or U-series (Soligo et al., 2002; Uysal et al., 2007; Sierralta et al., 2010; Nishikawa et al., 2012; Gao et al., 2013).

Finally, the results and findings from the present study lead us to suggest that changes in Ca isotopic compositions in oceanic and continental carbonates, formed with a set of environmental conditions similar to those from Baishuitai ($[Ca^{2+}] \gg [CO_3^{2-}]$, $7.5 < pH < 9$ and $pCO_2 < 0.01$ atm) should help to give information about past variations of $\delta^{44/40}Ca_{aq}$.

6. Conclusions

The Ca isotopic compositions of the present-day travertine and associated solution in the canal and pools at Baishuitai (Yunnan, SW China) were investigated to identify the mechanisms controlling Ca isotope fractionations. In each system, $\delta^{44/40}Ca$ values of the solution and travertine exhibited in-phase downstream increases. Isotopically light Ca is preferentially removed from the solution, leaving the remaining aqueous Ca^{2+} enriched in heavy isotopes.

The negative correlation between $\Delta^{44/40}Ca_{CaCO3\text{-}aq}$ values and the travertine precipitation rates in this study is in accordance with the results of previous experimental studies (Tang et al., 2008, 2012). This negative correlation can be explained using the theoretical steady-state surface kinetic model from DePaolo (2011), which suggests an equilibrium isotopic fractionation factor close to 1 ($\alpha_{eq} = 1.0000 \pm 0.0001$) and a kinetic fractionation factor associated with precipitation equal to 0.9983 ± 0.0002. These values are similar within error bars to those obtained for calcium carbonate precipitated in other continental contexts (Nielsen and DePaolo, 2013) and in the laboratory (Tang et al., 2008). Another consequence of this article is that Ca isotopes measured in travertine samples are representative of the Ca isotopic signature of the surrounding water, itself directly dependent on the amount of precipitated Ca. Consequently, Ca isotopes could be a good tool to reconstruct past hydrodynamic variations in travertine core samples.

Table EA.2
Hydrochemical compositions of the canal and pool waters from Baishuitai travertine site.

Site	Sampling date	K^+ (mmol/L)	Na^+ (mmol/L)	Mg^{2+} (mmol/L)
Canal system				
S1-3	28–07-2010	0.017	0.13	0.49
	28–01–2012	u.d.	0.05	0.21
W1	28–07-2010	0.017	0.12	0.51
	28–01–2012	u.d.	0.08	0.32
W2	28–07-2010	0.008	0.10	0.43
	28–01–2012	u.d.	0.09	0.37
W3	28–07-2010	0.008	0.10	0.43
	28–01–2012	u.d.	0.06	0.25
W4	28–07-2010	0.012	0.10	0.44
	28–01–2012	u.d.	0.07	0.29
W5	28–07-2010	0.017	0.12	0.49
	28–01–2012	0.002	0.09	0.36
Pool system				
S1-1	28–07-2010	0.033	0.39	0.66
	28–01–2012	0.008	0.19	0.65
P4	28–07-2010	0.028	0.33	0.62
	28–01–2012	0.014	0.23	0.76
P4.5	28–01–2012	0.009	0.19	0.66
P5	28–07-2010	0.028	0.32	0.59
	28–01–2012	0.011	0.21	0.68

u.d.: under detection limit.

Acknowledgement

This study was supported by the National Natural Science Foundation of China (Grant Nos. 41172232, 41372263, 41430753, and U1301231) and the National Basic Research Program of China (Grant No. 2013CB956703). It has also been financially supported by REALISE (REseau Alsace de Laboratoires en Ingéniérie et Sciences pour l'Environnement). Jiubin Chen, Zaihua Liu and Hao Yan acknowledge the funding of "Caiyuanpei" project by China Scholarship Council. A.-D. Schmitt wants to acknowledge Damien Daval for fruitful discussions about carbonate precipitation and dissolution rates. A.-D. Schmitt and F. Chabaux sincerely thank Peter Stille for many productive conversations. This article benefited from the constructive reviews of an anonymous reviewer and M. S. Fantle. We thank M.E. Böttcher for editorial handling.

References

Andrews, J.E., 2006. Palaeoclimatic records from stable isotopes in riverine tufas: synthesis and review. Earth Sci. Rev. 75, 85–104.
Andrews, J.E., Brasier, A.T., 2005. Seasonal records of climatic change in annually laminated tufas: short review and future prospects. J. Quat. Sci. 20, 411–421.
Chafetz, H., Rush, P.F., Utech, N.M., 1991. Microenvironmental controls on mineralogy and habit of $CaCO_3$ precipitates: an example from an active travertine system. Sedimentology 38, 107–126.
Chou, L., Garrels, R.M., Wollast, R., 1989. Comparative study of the kinetics and mechanisms of dissolution of carbonate minerals. Chem. Geol. 78, 269–282.
Cobert, F., Schmitt, A.D., Bourgeade, P., Labolle, F., Badot, P.-M., Chabaux, F., Stille, P., 2011. Experimental identification of Ca isotopic fractionations in higher plants. Geochim. Cosmochim. Acta 75, 5467–5482.
Crossey, L.J., Karlstrom, K.E., Springer, A.E., Newell, D., Hilton, D.R., Fischer, T., 2009. Degassing of mantle-derived CO_2 and He from springs in the southern Colorado plateau region—neotectonic connections and implications for groundwater systems. Geol. Soc. Am. Bull. 121, 1034–1053.
DePaolo, D., 2011. Surface kinetic model for isotopic and trace element fractionation during precipitation of calcite from aqueous solutions. Geochim. Cosmochim. Acta 75, 1039–1056.
Dietzel, M., Tang, J., Leis, A., Kohler, S.J., 2009. Oxygen isotopic fractionation during inorganic calcite precipitation-effects of temperature, precipitation rate and pH. Chem. Geol. 268, 107–115.
Eisenhauer, A., Nagler, T., Stille, P., Kramers, J., Gussone, N., Bock, B., Fietzke, J., Hippler, D., Schmitt, A.D., 2004. Proposal for an international agreement on Ca notations resulting from discussions at workshops on stable isotope measurements held in Davos (Goldschmidt 2002) and nice (EGS AGU EUG 2003). Geostand. Geoanal. Res. 28, 149–151.
Fantle, M.S., DePaolo, D.J., 2007. Ca isotopes in carbonate sediment and pore fluid from ODP site 807 A: the Ca^{2+}(aq)–calcite equilibrium fractionation factor and calcite recrystallization rates in Pleistocene sediments. Geochim. Cosmochim. Acta 71, 2524–2546.
Ford, T.D., Pedley, H.M., 1996. A review of tufa and travertine deposits of the world. Earth Sci. Rev. 41, 117–175.

Gao, J., Zhou, X., Fang, B., Li, T., Tang, L., 2013. U-series dating of the travertine depositing near the rongma hot springs in Northern Tibet, China, and its paleoclimatic implication. Quat. Int. 298, 98–106.
Gussone, N., Eisenhauer, A., Heuser, A., Dietzel, M., Bock, B., Böhm, F., Spero, H.J., Lea, D.W., Bijma, J., Nägler, T.F., 2003. Model for kinetic effects on calcium isotope fractionation (δ^{44}Ca) in inorganic aragonite and cultured planktonic foraminifera. Geochim. Cosmochim. Acta 67, 1375–1382.
Gussone, N., Böhm, F., Eisenhauer, A., Dietzel, M., Heuser, A., Teichert, B.M.A., Reitner, J., Worheide, G., Dullo, W.C., 2005. Calcium isotope fractionation in calcite and aragonite. Geochim. Cosmochim. Acta 69, 4485–4494.
Gussone, N., Nehrke, G., Teichert, B., 2011. Calcium isotope fractionation in ikaite and vaterite. Chem. Geol. 285, 194–202.
Harouaka, K., Eisenhauer, A., Fantle, M.S., 2014. Experimental investigation of Ca isotopic fractionation during abiotic gypsum precipitation. Geochim. Cosmochim. Acta 129, 157–176.
Hori, M., Ishikawa, T., Nagaishi, K., Lin, K., Wang, B., You, C., Shen, C., Kano, A., 2013. Prior calcite precipitation and source mixing process influence Sr/Ca, Ba/Ca and ^{87}Sr/^{86}Sr of a stalagmite developed in Southwestern Japan during 18.0–4.5 ka. Chem. Geol. 347, 190–198.
Hippler, D., Schmitt, A.D., Gussone, N., Heuser, A., Stille, P., Eisenhauer, A., Nägler, T.F., 2003. Calcium isotopic composition of various reference materials and seawater. Geostand. Newslett. 27, 13–19.
Ihlenfeld, C., Norman, M.D., Gagan, M.K., Drysdale, R.N., Maas, R., Webb, J., 2003. Climatic significance of seasonal trace element and stable isotope variations in a modern freshwater tufa2. Geochim. Cosmochim. Acta 67, 2341–2357.
Jacobson, A.D., Holmden, C., 2008. δ^{44}Ca evolution in a carbonate aquifer and its bearing on the equilibrium isotope fractionation factor for calcite. Earth Planet. Sci. Lett. 270, 349–353.
Jones, B., Renaut, R.W., 2010. Calcareous spring deposits in continental settings. Dev. Sedimentol. 61, 177–224.
Kano, A., Matsuoka, J., Kojo, T., Fujii, H., 2003. Origin of annual laminations in tufa deposits, Southwest Japan. Palaeogeogr. Palaeoclimatol. Palaeoecol. 191, 243–262.
Kano, A., Hagiwara, R., Kawai, T., Hori, M., Matsuoka, J., 2007. Climatic conditions and hydrological change recorded in a high-resolution stable-isotope profile of a recent laminated tufa on a subtropical island, Southern Japan. J. Sediment. Res. 77, 59–67.
Kawai, T., Kano, A., Hori, M., 2009. Geochemical and hydrological controls on biannual lamination of tufa deposits. Sediment. Geol. 213, 41–50.
Lemarchand, D., Wasserburg, G., Papanastassiou, D., 2004. Rate-controlled calcium isotope fractionation in synthetic calcite. Geochim. Cosmochim. Acta 68, 4665–4678.
Liu, Z., Zhang, M., Li, Q., You, S., 2003. Hydrochemical and isotope characteristic of spring water and travertine in the Baishuitai area (SW China) and their meaning for paleoenvironmental reconstruction. Environ. Geol. 44, 698–704.
Liu, Z., Li, H., You, C., Wan, N., Sun, H., 2006. Thickness and stable isotopic characteristics of modern seasonal climate-controlled sub-annual travertine laminas in a travertine-depositing stream at Baishuitai, SW China: implications for paleo-climate reconstruction. Environ. Geol. 51, 257–265.
Liu, Z., Sun, H., Lu, B., Liu, X., Ye, W., Zeng, C., 2010. Wet-dry seasonal variations of hydrochemistry and carbonate precipitation rates in a travertine-depositing canal at Baishuitai, Yunnan, SW China: implications for the formation of biannual laminae in travertine and for climatic reconstruction. Chem. Geol. 273, 258–266.
Marriott, C.S., Henderson, G.M., Belshaw, N.S., Tudhope, A.W., 2004. Temperature dependence of δ^{7}Li, δ^{44}Ca and Li/Ca during growth of calcium carbonate. Earth Planet. Sci. Lett. 222, 615–624.
Matsuoka, J., Kano, A., Oba, T., Watanabe, T., Sakai, S., Seto, K., 2001. Seasonal variation of stable isotopic compositions recorded in a laminated tufa, SW Japan. Earth Planet. Sci. Lett. 192, 31–44.
Minissale, A., Kerrick, D.M., Magro, G., Murrell, M.T., Paladini, M., Rihs, S., Sturchio, N.C., Tassi, F., Vaselli, O., 2002. Geochemistry of quaternary travertines in the region north of Rome (Italy): structural, hydrologic and paleoclimatic implications. Earth Planet. Sci. Lett. 203, 709–728.
Nielsen, L.C., DePaolo, D.J., Yoreo, J.J.D., 2012. Self-consistent ion-by-ion growth model for kinetic isotope fractionation during calcite precipitation. Geochim. Cosmochim. Acta 86, 166–181.
Nielsen, L.C., DePaolo, D.J., 2013. Ca isotope fractionation in a high-alkalinity lake system: mono Lake, California. Geochim. Cosmochim. Acta 118, 276–294.
Nishikawa, O., Furuhashi, K., Masuyama, M., Ogata, T., Shiraishi, T., Shen, C.-C., 2012. Radiocarbon dating of residual organic matter in travertine formed along the yumoto fault in oga peninsula, Northeast Japan: implications for long-term hot spring activity under the influence of earthquakes. Sediment. Geol. 243-244, 181–190.
Parkhurst, D.L., Appelo, C.A.J., 1999. User's guide to PHREEQC-a computer program for speciation, batch-reaction, one-dimensional transport, and inverse geochemical calculations. U.S. Geol. Surv. Water Resour. Invest., 99–4259.
Pentecost, A., 2005. Travertine. Springer-Verlag, Berlin and Heidelberg (445 pp).
Plummer, L.N., Wigley, T.M.L., Parkhurst, D.L., 1978. The kinetics of calcite dissolution in CO_2-water systems at 5–60 °C and 0.0–1.0 atm CO_2. Amer. J. Sci. 278, 179–216.
Pokrovsky, O.S., Golubev, S.V., Schott, J., Castillo, A., 2009. Calcite, dolomite and magnesite dissolution kinetics in aqueous solutions at acid to circumneutral pH, 25 to 150 °C and 1 to 55 atm pCO_2: new constraints on CO_2 sequestration in sedimentary basins. Chem. Geol. 265, 20–32.
Reynard, L.M., Day, C.C., Henderson, G.M., 2011. Large fractionation of calcium isotopes during cave-analogue calcium carbonate growth. Geochim. Cosmochim. Acta 75, 3726–3740.
Ryu, J.-S., Jacobson, A., Holmden, C., Lundstrom, C., Zhang, Z., 2011. The major ion, $\delta^{44/40}$Ca, $\delta^{44/42}$Ca, and $\delta^{26/24}$Mg geochemistry of granite weathering at pH = 1 and T = 25 °C: power-law processes and the relative reactivity of minerals. Geochim. Cosmochim. Acta 75, 6004–6026.
Schmitt, A.D., Gangloff, S., Cobert, F., Lemarchand, D., Stille, P., Chabaux, F., 2009. High performance automated ion chromatography separation for Ca isotope measurements in geological and biological samples. J. Anal. At. Spectrom. 24, 1089–1097.
Schmitt, A.D., Cobert, F., Bourgeade, P., Ertlin, D., Labolle, F., Gangloff, S., Badot, P.M., Chabaux, F., Stille, P., 2013. Calcium isotope fractionation during plant growth under limiting nutrient supply. Geochim. Cosmochim. Acta 110, 70–83.
Sierralta, M., Kele, S., Melcher, F., Hambach, U., Reinders, J., van Geldern, R., Frechen, M., 2010. Uranium-series dating of travertine from Süttő: implications for reconstruction of environmental change in Hungary. Quat. Int. 222, 178–193.
Soligo, M., Tuccimei, P., Barberi, R., Delitala, M.C., Miccadei, E., Taddeucci, A., 2002. U/Th dating of freshwater travertine from middle Velino Valley (Central Italy): paleoclimatic and geological implications. Palaeogeogr. Palaeoclimatol. Palaeoecol. 184, 147–161.
Sun, H., Liu, Z., 2010. Wet-dry seasonal and spatial variations in the δ^{13}C and δ^{18}O values of the modern endogenic travertine at Baishuitai, Yunnan, SW China and their paleoclimatic and paleoenvironmental implications. Geochim. Cosmochim. Acta 74, 1016–1029.
Sun, H., Liu, Z., Yan, H., 2014. Oxygen isotope fractionation in travertine-depositing pools at Baishuitai, Yunnan, SW China: effects of deposition rates. Geochim. Cosmochim. Acta 133, 340–350.
Tang, J., Dietzel, M., Böhm, F., Kohler, S., Eisenhauer, A., 2008. Sr^{2+}/Ca^{2+} and ^{44}Ca/^{40}Ca fractionation during inorganic calcite formation: II. Ca isotopes. Geochim. Cosmochim. Acta 72, 3733–3745.
Tang, J., Niedermayr, A., Köhler, S.J., Böhm, F., Kisakürek, B., Eisenhauer, A., Dietzel, M., 2012. Sr^{2+}/Ca^{2+} and ^{44}Ca/^{40}Ca fractionation during inorganic calcite formation: III. impact of salinity/ionic strength. Geochim. Cosmochim. Acta 77, 432–443.
Tipper, E.T., Galy, A., Bickle, M.J., 2006. Riverine evidence for a fractionated reservoir of Ca and Mg on the continents: implications for the oceanic Ca cycle. Earth Planet. Sci. Lett. 247, 267–279.
Uysal, I.T., Feng, Y., Zhao, J.-X., Altunel, E., Weatherley, D., Karabacak, V., Cengiz, O., Golding, S.D., Lawrence, M.G., Collerson, K.D., 2007. U-series dating and geochemical tracing of late quaternary travertine in co-seismic fissures. Earth Planet. Sci. Lett. 257, 450–462.
Wang, H., Yan, H., Liu, Z., 2014. Contrasts in variations of the carbon and oxygen isotopic composition of travertines formed in pools and a ramp stream at huanglong ravine, China: implications for paleoclimatic interpretations. Geochim. Cosmochim. Acta 125, 34–48.
Watson, E.B., 2004. A conceptual model for near-surface kinetic controls on the trace-element and stable isotope composition of abiogenic calcite crystals. Geochim. Cosmochim. Acta 68, 1473–1488.
Yan, H., Sun, H., Liu, Z., 2012. Equilibrium vs. kinetic fractionation of oxygen isotopes in the two low-temperature travertine-depositing systems with distinct hydrodynamic conditions at Baishuitai, Yunnan SW China. Geochim. Cosmochim. Acta 95, 63–78.
Zuddas, P., Mucci, A., 1994. Kinetics of calcite precipitation from seawater: I. A classical chemical kinetics description for strong electrolyte solutions. Geochim. Cosmochim. Acta 58, 4353–4362.